

Humic acid-, ferrihydrite-, and aluminosilicate-coated sands for column transport experiments

Jorge Jerez, Markus Flury*

Department of Crop and Soil Sciences and Department of Biological Systems Engineering, Center for Multiphase Environmental Research, Washington State University, Pullman, WA 99164, USA

Received 2 June 2005; received in revised form 18 July 2005; accepted 5 August 2005

Available online 16 September 2005

Abstract

Interactions of chemicals with soil minerals are often studied in batch systems. Dynamic flow systems are often limited by the low hydraulic permeability of the soil constituents, such as clays, when packed into columns. However, if clay minerals and organic matter can be immobilized on an inert support, then dynamic flow experiments can be performed. In this study, we investigate the feasibility to produce porous media with similar hydrodynamic properties, but different surface characteristics. Four minerals (ferrihydrite, kaolinite, illite, and smectite) and a humic acid were coated on silica sand grains. Coated grains were packed into columns and the hydrodynamic properties of the media were determined with anionic tracers. The hydrodynamic properties of the various coated silica sands were similar, suggesting that porous media with similar spatial structure, but different surface characteristics, could be produced. Coating of clay minerals was shown to cause anion exclusion of anionic tracers when high surface charge clays or high clay loadings for the coating procedure were used. The specific surface area of the coating materials inside the porous medium could be changed by varying the particle size of the silica grain support. Coating of different materials onto silica sand grains allows to study interactions of chemicals and colloids with dynamic flow experiments in a porous medium with defined structure.

© 2005 Elsevier B.V. All rights reserved.

Keywords: Silica sand; Ferrihydrite; Smectite; Illite; Kaolinite; Humic acid; Breakthrough; Transport

1. Introduction

Clays, organic matter, and iron- and aluminum-oxides, are the most reactive solid constituents in soils and sediments. These materials play a major role in the fate and transport of contaminants. Studies with pure minerals have provided mechanistic insight about solid–liquid phase interactions of a variety of chemicals with mineral surfaces [1]. Batch sorption experiments are standard methods for studying interactions of chemicals with soils and sediments, and to derive sorption coefficients and equilibrium constants. An alternative approach to derive the latter parameters are column transport experiments. Column transport experiments have certain advantages over batch sorption studies, i.e., the experimental conditions may be more representative of natural conditions in a flow-through column than in a batch reactor. However, many solid materials are not suitable for

column experiments, because of their small particle size which may cause columns to clog up [2]. Coating of such materials on an inert support, such as sand or glass beads, would allow performing column transport experiments with a structurally stable and hydraulically conductive porous medium.

Iron-oxides have been successfully coated on silica sand particles [3,4] and used for studying humic acid interactions with iron-oxides [5] and the transport of heavy metals [6] and radionuclides [7]. Similarly, humic acids have been immobilized on silica to obtain porous materials suitable for sorption studies [8–11]. Humic acid can also be immobilized in a porous matrix using a soil-gel process, whereby a glassy matrix is produced through a series of hydrolysis and polymerization reactions [12]. It has recently been shown that clay minerals can be coated on silica sand and glass beads [13,14].

The possibility to coat silica sands or glass beads with iron-oxides, humic material, and clay minerals offers the opportunity to study the interactions of solutes with three major soil constituents using dynamic column experiments. If the soil constituents are coated on the same silica sand or glass bead matrix,

* Corresponding author. Tel.: +1 509 335 1719; fax: +1 509 335 8674.

E-mail address: flury@mail.wsu.edu (M. Flury).

then we can construct porous media which have similar structure, but different surface characteristics.

The objective of this work was to investigate the hydrodynamic properties of porous materials (packed silica sand) coated with different soil constituents. We hypothesized that we can construct porous media with identical hydrodynamic properties, but different surface characteristics. Furthermore, we tested whether we can modify the hydraulic properties without changing the surface characteristics of the medium. Our approach was to coat silica sand with humic acid, ferrihydrite, or clay minerals, and to compare the transport of anionic tracers through columns packed with coated sand material.

2. Materials and methods

2.1. Silica sand and sand pretreatment

Silica sand (J.T. Baker, Phillipsburg, NJ; CAS No. 14808-60-7) was fractionated by dry sieving to obtain particles between 0.25 and 1 mm diameter. The sand was treated with H₂O₂ to remove organic matter [15] and with citrate-dithionite to remove iron [16]. Then the sand was extensively rinsed with deionized water and oven dried at 110 °C.

2.2. Humic acid coating of silica sand

Humic acid was obtained from Aldrich (Lot No. 03130JS). We coated the humic acid over the silica sand following the methodology developed by Koopal et al. [10]. This procedure involved modification of the silica surface with 3-aminopropyltriethoxysilane (APTS) (Aldrich, MI) [10,11,17]. We specifically used the incubation with *N*-(3-dimethylaminopropyl)-*N'*-ethylcarbodiimide hydrochloride (EDC) at room temperature, and then followed by end-capping of the free amino groups as described in Koopal et al. [10]. Multilayer-coating is obtained when the APTS reaction is not carried out with a completely anhydrous medium [11]. We did not use completely anhydrous conditions during the reactions of APTS with the silica, to obtain as much humic acid coating as possible. This resulted in multilayer humic acid coatings in our samples.

The amount of humic acid coated on the sand was determined by detachment of the humic acid in 1 M NaOH followed by quantification with UV–vis spectrometry (HP 8452A, Hewlett-Packard) at a wavelength of 254 nm. The spectroscopic measurements were calibrated with a TOC analyzer (TOC 5000, Shimadzu Corporation, Kyoto, Japan).

2.3. Ferrihydrite coating of silica sand

Ferrihydrite (6-line ferrihydrite) was synthesized according to Schwertmann and Cornell [4]. For the synthesis, Pyrex glass beakers were used. After synthesis, the ferrihydrite was dialyzed at room temperature (20–22 °C) until the electrical conductivity of the solution was less than 5 μS/cm.

We coated the silica sand with ferrihydrite using a slightly modified procedure developed by Scheidegger et al. [3]. We carried out initial experiments to test optimal concentration and

pH at which a homogeneous and extensive coating of silica sand with ferrihydrite was obtained. Briefly, 40 mL dialyzed ferrihydrite suspension was mixed with 60 g silica sand, and shaken for a total of 3 days. The pH of the initial solution was 6.5, and after 1 day of shaking, the pH was adjusted to 7.0 with 0.01 M NaOH, and after another day to pH 7.5. Finally, the sand was washed three times with 1 M HNO₃ and 10 M NaOH. The amount of Fe coated over the sand was determined by dissolution of ferrihydrite with 2 M HCl at 80 °C for 12 h, followed by quantification of Fe by Atomic Absorption Spectroscopy (Varian 220 Flame Atomic Absorption Spectrometer). The mineralogical stability of ferrihydrite was verified with X-ray diffraction (Philips XRG 3100, Philips Analytical Inc., Mahwah, NJ).

2.4. Aluminosilicate coating of silica sand

Four clay minerals, Georgia kaolinite (KGa1), Arizona smectite (SAz1), Texas smectite (STx1) (Source Clay Minerals Repository, University of Missouri), and illite (No. 36, Morris, Illinois, Ward's Natural Science, Rochester, NY) were selected to be coated over the sand. The clay minerals were treated to remove organic matter using H₂O₂ [15] and iron oxides using citrate-dithionite [16] and were then fractionated to obtain particles <2 μm in hydrodynamic diameter using gravity sedimentation. The clay minerals were made homoionic by washing with 1 M NaCl (KGa1), 0.5 M CaCl₂ (SAz1 and STx1) or 1 M KCl (Illite) [18]. Finally, the clays were dialyzed with deionized water until the electrical conductivity of the solution was less than 5 μS/cm.

The clay minerals were coated over the sand surface using the procedures described in detail in Jerez et al. [14]. Briefly, clay suspensions were flocculated with 50 mg/L polyacrylamide (Superfloc C498, Cytec Industries, West Paterson, NJ). The mixture was then left to settle down, and centrifuged at 100 × *g* for 5 min. Then, the clay–polymer complex slurry was mixed with the silica sand and dried at 100 °C for 24 h. The coated sand was then washed with deionized water and dried again at 100 °C for 24 h. The washing removed all non-attached polyacrylamide. The amount of clay coated over the silica sand was determined by detaching the clays with 1 M NaOH, followed by clay quantification with UV–vis spectrometry at 230-nm wavelength.

We chose the different clay minerals to represent major types of aluminosilicate clays. The two smectites differed with respect to surface charge. The cation exchange capacity (CEC) of SAz1 (123 ± 3 mmol_c/100 g) is around 40% greater than that of STx1 (89 ± 2 mmol_c/100 g) [19]. This allowed us to assess the effect of surface charge on transport of anionic tracers.

2.5. Surface characterization of soil constituents and coated sands

Specific surface areas were determined with N₂ adsorption (ASAP2010, Micromeritics, Norcross, GA) based on BET isotherms. We measured the surface areas of the minerals and humic acid before coating onto the sands, and then measured the surface areas of the coated sands. The isoelectric point (IEP) for ferrihydrite and kaolinite was measured in a 1 mM

NaCl background with dynamic light scattering (Zetasizer 3000 HSA, Malvern Instruments Ltd., Malvern, UK). For kaolinite-, ferrihydrite-, and humic acid-coated sands, the point of zero salt effect (PZSE) was measured by the salt addition method [6]. About 20 g of the coated material was packed into a column, and 20 mL of 0.01 M NaNO₃ was recirculated at a rate of four pore volumes per minute. The pH was monitored with a flow-cell electrode. When the pH was equilibrated, 0.4 mL of 5 M NaNO₃ was added to increase the salt concentration by a factor of 10, and the pH change was monitored. This was done with initial pH values ranging from 2 and 9. The PZSE was obtained when no pH change was observed after the addition of the high concentration salt solution. Although the IEP and the PZSE are different and cannot be directly compared [20], they give indication about the overall surface charge characteristics of the particles. The surface morphology of the coated sands was examined by scanning electron microscopy (Hitachi S520, Hitachi Instruments, Inc., Tokyo, Japan).

2.6. Column transport experiments

Column experiments were performed in a borosilicate glass column of 1.5-cm diameter and 12-cm length (Omnifit, Cambridge, UK). The column end pieces consisted of Teflon frits of 40 μm pore diameter. The column was packed with clean or coated sands under saturated condition. The solution background was chosen to mimic a soil pore water solution [21] and consisted of an electrolyte mixture with 4.45 mM CaCl₂, 1.4 mM MgCl₂, 0.4 mM KCl, 0.7 mM and NaCl, with an ionic strength of 18.55 mM. The background solution was pumped through the column from the bottom using a peristaltic pump (Ismatec, Switzerland). At least 20 pore volumes were flushed through the column to equilibrate the system before the tracer experiment.

Column breakthrough curves were determined using nitrate (0.2 mM NaNO₃) or bromide (0.2 mM KBr) as tracers spiked to the background electrolyte solution. The tracer concentration was measured online with a flow cell and a diode array spectrophotometer; NO₃⁻ was measured at a wavelength of 220 nm and Br⁻ at 202 nm. Calibrations of tracer standards followed Beer's law. Tracers were fed into the column as pulses of two to four pore volumes.

Column breakthrough curves were analyzed to determine the pore water velocity v and the hydrodynamic dispersion coefficient D using the advection–dispersion equation (ADE) and the code CXTFIT [22]. The Peclet number, Pe , was calculated as $Pe = vL/D$, where L is the length of the column.

Three different sets of experiments were conducted. A constant flow rate of 1.2 mL/min was used for all experiments. In the first set, we evaluated the hydrodynamic dispersion of the coated sands (humic acid, ferrihydrite, kaolinite, illite and Texas Ca-smectite-coated silica sands). The second set of experiments was used to evaluate the effect of grain size of the coated sands on the hydrodynamic properties of the porous materials. For these experiments, we fractionated the Texas-smectite-coated sand by sieving into two fractions, with particle diameters from 255 to 355 and 425 to 500 μm, respectively. The third set of experi-

ments was used to investigate the behavior of an anionic tracer in ferrihydrite-coated sand, and two types of high-load smectite-coated sands. The high-load coated sands were obtained by using the polyvinyl alcohol methodology described by Jerez et al. [14]. Each breakthrough curve was repeated at least twice. Replicates were reproducible (tracer concentrations deviated less than 2%; porosity and flow rates deviated less than 3% between replicates), and we therefore only show one breakthrough curve for each experiment.

3. Results and discussion

3.1. Surface characterization of coated sands

Fig. 1 shows images of coated silica sand surfaces. The clean silica surface depicts an irregular topography (Fig. 1A). The coatings covered the silica surface incompletely, there were always some portions of the surface that were not covered by the coatings. Based on screenings of the images, we estimate that about 80% of the surface was covered by coatings. Incomplete surface coating of iron-oxides was also observed by others [3].

Quantitative characteristics of the coated sands are listed in Table 1. The amount of humic material and minerals that could be coated onto the silica grains was in the range of 1–25 mg/g of sand, except for the clay coating with the polyvinyl alcohol method, which resulted in higher surface coverage. The coated sands had a PZSE similar to that of the coating materials. The specific surface areas of the coated sands were about two orders of magnitude smaller than the surface areas of the coating materials itself, but considerably larger than that of the uncoated sand. The amount of coating per surface area was calculated from the measured specific surface area and the amount of coating per mass.

The amount of humic acid that we could coat onto the sand was around 1 mg/g of sand (Table 1), which is similar to the result obtained using sol-gel immobilization [12]. Koopal et al. [10] reported a surface coverage of humic acid of 56 mg/g, but used a much smaller-sized silica support than we did. On a per surface area basis, our 26 mg/m² compares with 1.1 mg/m² from Koopal et al. [10]. The higher surface loading obtained in our experiments is likely due to multilayer coverage (Fig. 1B), compared to monolayer coverage in Koopal et al. [10].

The amount of ferrihydrite coating was 4.4 mg Fe/g, which is in the range reported previously [3]. The IEP for the ferrihydrite mineral was pH 6.8, which is low for iron oxides but can be explained by inclusion of small amounts of silica [23]. The surface area of the coated sand was one order magnitude larger than that of the clean sand, in agreement with published data [6]. The specific surface area of ferrihydrite (65 m²/g) was smaller than that reported by Negre et al. [24] (301 m²/g). X-ray diffraction measurements confirmed the presence and stability of 6-line ferrihydrite before and after coating.

Aluminosilicate clays coated on silica sand using the polyacrylamide method had similar specific surface areas as the iron-oxide-coated sand (Table 1). A one order magnitude larger surface area was obtained for sand coated with polyvinyl alcohol. For the aluminosilicate clays, the IEP was only determined

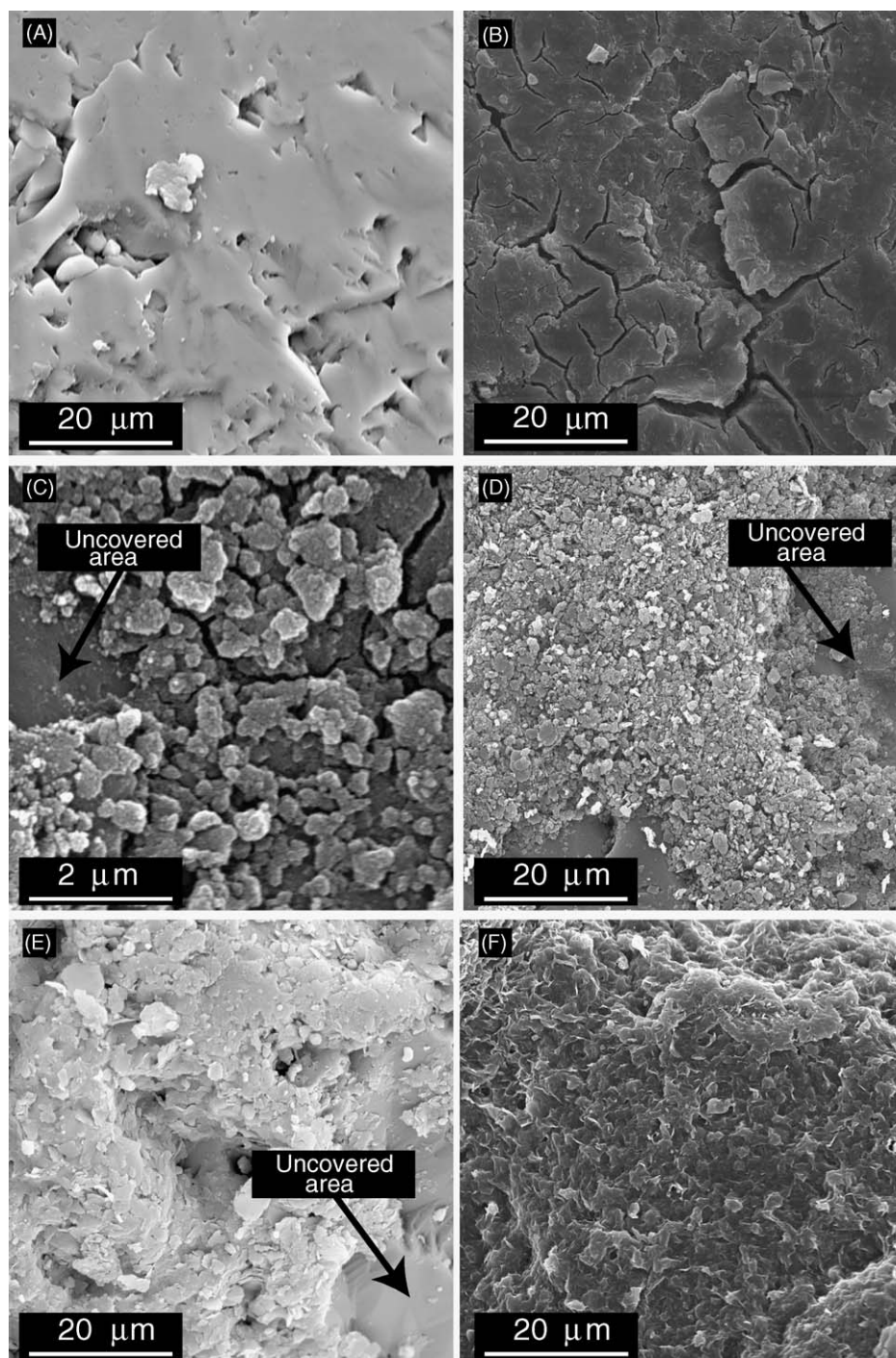


Fig. 1. Scanning electron micrographs of (A) clean silica sand (control), (B) humic acid-coated sand, (C) ferrihydrite-coated sand, (D) kaolinite-coated sand (KGa1), (E) illite-coated sand (No. 36, Morris), and (F) smectite-coated (STx1) sand. Note that the scale of the ferrihydrite micrograph is different than the other scales. The “uncovered areas” show the silica sand surface.

for kaolinite, but not for illite and smectite which have a permanent structural negative charge. The IEP for kaolinite minerals was pH 2.4, and the PZSE of kaolinite-coated sand was pH 2.9.

3.2. Column transport experiments

Fig. 2 shows breakthrough curves of anionic tracers in coated sand media. Nitrate did not behave as conservative (non-

reactive) tracer in ferrihydrite-coated sand. We used Br^- as tracer, which behaved conservatively at pH 9.9. The breakthrough curves could be well described by the ADE for a conservative chemical, and the model parameters are listed in Table 2. Measured and estimated pore water velocities were very similar. The different coated sands had similar hydrodynamic dispersion coefficients and Peclet numbers, indicating that all porous media possessed similar hydrodynamic properties. This shows that we

Table 1
Characteristics of humic acid, minerals, and coated sands

Material	Specific surface area (m ² /g)	IEP/PZSE ^a (pH)	Amount of coating	
			In mg/g	In mg/m ²
Coating materials				
Humic acid (Aldrich)	5.9 ± 0.3 ^b	na ^c	None	None
Ferrihydrite	65.3 ± 0.8	6.8	None	None
Kaolinite (KGa1)	13.6 ± 0.3	2.4	None	None
Illite (No. 36, Morris)	36.5 ± 0.4	None	None	None
Texas smectite (STx1)	52.6 ± 0.5	None	None	None
Arizona smectite (SAz1)	25.1 ± 0.9	None	None	None
Sands				
Control, uncoated sand	0.04 ± 0.001	3.2	None	None
Humic acid-coated sand	0.21 ± 0.01	3.4	1.04 ± 0.03	26
Ferrihydrite-coated sand	0.4 ± 0.01	6.7	4.4 ± 0.2	109
Kaolinite-coated sand	0.24 ± 0.01	2.9	24.7 ± 3.2	618
Illite-coated sand	0.29 ± 0.01	None	5.0 ± 0.4	126
Smectite (STx1)-coated sand (low-load)	0.35 ± 0.01	None	3.1 ± 0.2	77
Smectite (STx1)-coated sand (high-load) ^d	2.41 ± 0.02	None	32.3 ± 3.5	808
Smectite (SAz1)-coated sand (high-load) ^d	1.20 ± 0.01	None	54.1 ± 5.1	1354

^a IEP: isoelectric point of coating materials; PZSE: point of zero salt effect for sands.

^b Errors denote 1 S.D.

^c na: not available.

^d Clay coating using the polyvinyl alcohol methodology.

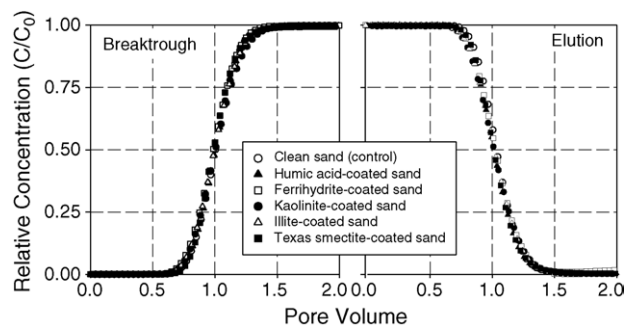


Fig. 2. Breakthrough curves of conservative tracers for different coated sands. In all cases NO₃⁻ was used as tracer, except for ferrihydrite-coated sand, where Br⁻ was used. The pH of the solutions was 6.5–7, except for ferrihydrite-coated sand, where the pH was 9.9.

can generate porous media with similar hydraulic properties, but different surface characteristics.

We used two anionic tracers, Br⁻ and NO₃⁻, to assess the hydrodynamic behavior of the coated sands. For ferrihydrite-

coated sands, we expected both Br⁻ and NO₃⁻ to be a conservative tracer when the solution pH was well above the IEP of ferrihydrite. A series of breakthrough curves conducted at different pH values showed that NO₃⁻ was retarded at pH 4.1, and as the pH was raised, the retardation became less and less (Fig. 3). However, even at pH ≈ 10, several pH units above the IEP of ferrihydrite, NO₃⁻ was retarded as compared to Br⁻, which behaved conservatively (Fig. 3). At pH 7.4, we also observed retardation of Br⁻, as would be expected because the ferrihydrite picks up more positive charges (data not shown). The observation that Br⁻ moved faster at high pH than NO₃⁻ may be attributed to different sorption characteristics of the two ions [25,26].

Anionic tracers may be subject to anion exclusion during transport in a porous medium that has highly negative surface charges [25]. Anion exclusion results in an early breakthrough of the anionic tracer, and has been observed repeatedly [27–29]. The higher the negative surface charge of the minerals, the more anion exclusion would be expected. We can readily demon-

Table 2
Summary of experimental and modeled breakthrough curves

Treatments	Measured		Fitted advection–dispersion equation (ADE) parameters			
	Porosity (%)	Pore water velocity (cm/min)	Pore water velocity (cm/min)	Hydrodynamic dispersion, D (cm ² /min)	Peclet number, Pe	R^2
Clean sand	35.1	1.97	1.95	0.25 ± 0.01 ^a	93 ± 4	0.999
Coated sands						
Humic acid	33.2	2.07	2.07	0.27 ± 0.03	91 ± 9	0.999
Ferrihydrite	36.4	1.82	1.87	0.24 ± 0.03	101 ± 11	0.988
Kaolinite (KGa1)	34.2	1.87	1.89	0.23 ± 0.01	99 ± 4	0.989
Illite	37.5	2.04	2.07	0.23 ± 0.02	102 ± 8	0.998
Smectite (STx1)	38.2	1.89	1.88	0.22 ± 0.02	104 ± 9	0.999

^a Errors denote 1 S.D.

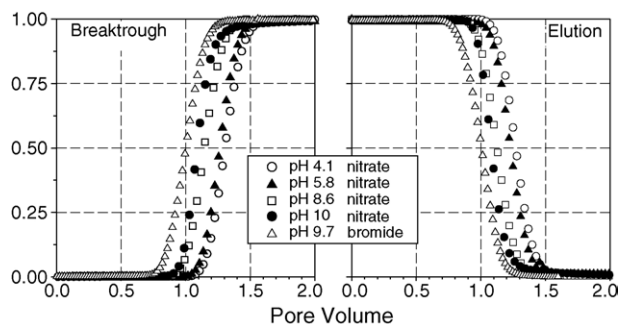


Fig. 3. Effect of pH on NO_3^- breakthrough curves in ferrihydrite-coated sand. The breakthrough curve for Br^- at pH 9.7 is shown as an example of a conservative tracer.

strate these effects using different clay loadings and differently charged clays (Table 1). Silica sand coated with a small amount of smectite (STx1-low-load) showed no anion exclusion, indicated by the superposition of its NO_3^- breakthrough with the one obtained in clean silica sand (Fig. 4). On the contrary, anion exclusion was observed for the high-load smectite-coated sand (STx1-high-load) as well as for the SAz1-smectite-coated sand; the breakthroughs occurred at 0.9 pore volumes as compared to at 1.0 pore volume for NO_3^- . Such anion exclusion effects may need to be considered when using high surface charge coatings.

The NO_3^- breakthrough curves in STx1-high-load and SAz1 smectite-coated sands were very similar (Fig. 4). The SAz1 smectite has a 40% higher CEC than the STx1 smectite [19], from which we would expect more anion exclusion in the SAz1-coated sand. However, the specific surface area of the SAz1-coated sand was about 50% less than that of the STx1-coated sand (Table 1). Consequently, the overall anion exclusion effect in these two porous media was similar.

Changing the grain size of the silica support allowed manipulation of the specific surface area of the coated porous medium as well as the amount of coating per unit mass of the porous medium. As an example, we show the coating of smectite (STx1) on silica grains with two different diameter ranges (Table 3). The specific surface area of the coated sand was doubled when the grain size of the support silica was reduced from 425–500 to 250–355 μm . A corresponding increase in the amount of clay coating per unit mass of porous medium was observed as well. The amount of clay coated per surface area of sand was similar, supporting that the increase in specific surface area was due to the

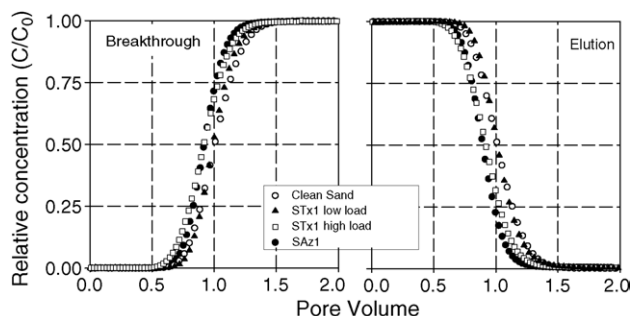


Fig. 4. Effect of clay loading on breakthrough curves of NO_3^- in smectite-coated sand.

Table 3

Effect of sand size on clay coverage for smectite (STx1)

Silica grains	Grain diameter (μm)	Specific surface area (m^2/g)	Clay coverage	
			In mg/g	In mg/m^2
Small grains	250–355	0.152 ± 0.007	15.7 ± 0.4	103 ± 7
Large grains	425–500	0.086 ± 0.004	11 ± 1	127 ± 21

The polyvinyl alcohol method described in Ref. [14] was used for the coating.

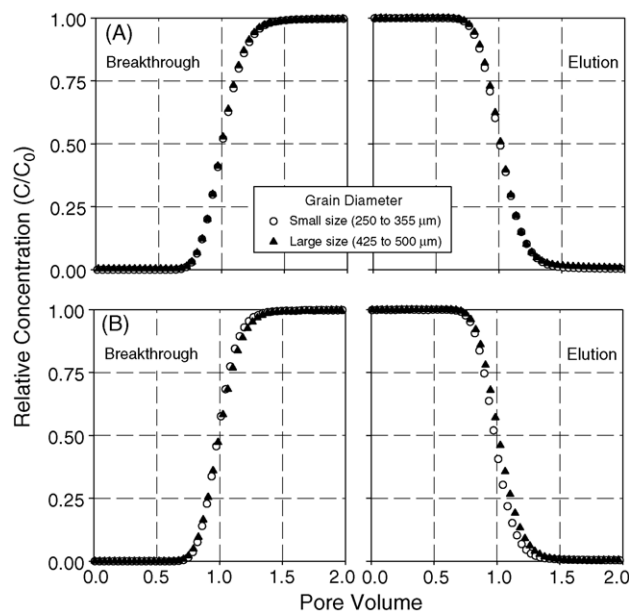


Fig. 5. Effect of sand particle size on breakthrough curves of NO_3^- . (A) Uncoated silica sand and (B) STx1-smectite-coated sand.

decrease in grain size. Fig. 5 illustrates that changing the grain size did not affect the hydrodynamic dispersion of the porous medium. The breakthrough curves of NO_3^- were similar among the two clay-coated sands, the uncoated sand, and also among the coated sands of different grain diameters. The hydrodynamic dispersion did not change; however, the hydraulic conductivity changed, because it is strongly dependent on the grain size of the medium [30,31].

4. Conclusions

Ferrihydrite-, aluminosilicate clay-, and humic acid-coated sand grains can be packed into columns and be used to study interactions of chemicals or colloids with the coating materials under dynamic flow conditions. Coated sand packings had the same hydrodynamic properties (Peclet numbers) as the uncoated sand packing. The coating of the silica grains allows to generate a permeable and structurally stable hydrodynamic system, yet with surface properties of colloidal-sized particles. Clay-coated silica sand media can cause anion exclusion, depending on the amount of clay coated onto the silica surfaces and the surface charge of the clays used. Such anion exclusion can be determined using a tracer breakthrough experiment. The specific surface area of the coating materials on the silica grain support can be manipulated by selecting different particle sizes of the silica

grains. The hydraulic conductivity of the system can be readily adjusted by selecting an appropriate particle size of the silica support grains.

Acknowledgements

This work was supported by the Washington State Water Research Center. We thank the Electron Microscopy Center at Washington State University for access to their facility.

References

- [1] W. Stumm, *Chemistry of the Solid-Water Interface*, John Wiley & Sons, New York, 1992.
- [2] R. Wibulswas, *Sep. Purif. Technol.* 39 (2004) 3.
- [3] A. Scheidegger, M. Borkovec, H. Sticher, *Geoderma* 14 (1993) 777.
- [4] U. Schwertmann, R.M. Cornell, *Iron Oxides in the Laboratory*, second ed., Wiley-VCH, Weinheim, Germany, 2000.
- [5] B. Gu, T.L. Mehlhorn, L. Liyuan, J.F. McCarthy, *Geochim. Cosmochim. Acta* 60 (1996) 2977.
- [6] M.M. Benjamin, R.S. Sletten, R.P. Bailey, T. Bennett, *Water Res.* 30 (1996) 2609.
- [7] B.O. Hansen, P. Kwan, M.M. Benjamin, G.V. Korshin, *Environ. Sci. Technol.* 35 (2001) 4905.
- [8] G. Szabo, P.S. Lesley, R.A. Bulman, *Chemosphere* 21 (1990) 729.
- [9] G. Szabo, R.A. Bulman, *J. Liquid Chromatogr.* 17 (1994) 2593.
- [10] L.K. Koopal, Y. Yang, A.J. Minnaard, P.L.M. Theunissen, W.H. Van Riemsdijk, *Colloids Surf. Physicochem. Eng. Aspects* 141 (1998) 385.
- [11] Y.-H. Yang, L.K. Koopal, *Colloids Surf. Physicochem. Eng. Aspects* 151 (1999) 201.
- [12] Y. Laor, C. Zolkov, R. Armon, *Environ. Sci. Technol.* 36 (2002) 1054.
- [13] C.L. Ake, K. Mayurana, G.R. Bratton, T.D. Phillips, *J. Toxicol. Environ. Health A* 63 (2001) 459.
- [14] J. Jerez, M. Flury, J. Shang, Y. Deng, *J. Colloid Interface Sci.*, in press.
- [15] G.W. Kunze, J.B. Dixon, Pretreatment of mineralogical analysis, in: A. Klute (Ed.), *Methods of Soil Analysis. Part 1. Physical and Mineralogical Analysis*, American Society of Agronomy, Madison, WI, 1986, pp. 91–100.
- [16] G.G.S. Holmgren, *Soil Sci. Soc. Am. Proc.* 31 (1967) 210.
- [17] K.C. Vrancken, K. Possemiers, E.F. Van Der Voort, E.F. Vansant, *Colloids Surf. Physicochem. Eng. Aspects* 98 (1995) 235.
- [18] H. van Olphen, *An Introduction to Clay Colloid Chemistry*, second ed., John Wiley, New York, 1977.
- [19] D. Borden, R.F. Giese, *Clays Clay Miner.* 49 (2001) 444.
- [20] G. Sposito, *Environ. Sci. Technol.* 32 (1998) 2815.
- [21] NRCS, Soil Data Mart Database (Whitman County, Washington), Natural Resources Conservation Service, 2005, online at <http://soildatamart.nrcs.usda.gov>, accessed May 2005.
- [22] N. Toride, F.J. Leij, M.T. van Genuchten, The CXTFIT Code for Estimating Transport Parameters from Laboratory or Field Experiments, Version 2.1, Research Report 137, U.S. Salinity Laboratory, Riverside, CA, 1995.
- [23] P.R. Anderson, M.M. Benjamin, *Environ. Sci. Technol.* 19 (1985) 1048.
- [24] M. Negre, P. Leone, C. Trichet, J. Defarge, V. Boero, M. Gennari, *Geoderma* 121 (2004) 1.
- [25] G. Sposito, *The Chemistry of Soils*, Oxford University Press, New York, 1989.
- [26] D.E. Clay, Z. Zheng, Z. Liu, S.A. Clay, T.P. Trooien, *J. Environ. Qual.* 33 (2004) 338.
- [27] R.S. Bowman, *Soil Sci. Soc. Am. J.* 48 (1984) 897.
- [28] R.V. James, J. Rubin, *Soil Sci. Soc. Am. J.* 50 (1986) 1142.
- [29] R. Schoen, J. Gaudet, T. Bariac, *J. Hydrol. (Amsterdam)* 215 (1999) 70.
- [30] P.A. Domenico, F.W. Schwartz, *Physical and Chemical Hydrogeology*, second ed., John Wiley & Sons, New York, 1998.
- [31] C.W. Fetter, *Contaminant Hydrogeology*, second ed., Prentice Hall, Upper Saddle River, NJ, 1999.